JOURNAL
OF THE
AMERICAN
CHEMICAL
SOCIETY

Exploring Ground-State Heterogeneity of Hypericin and Hypocrellin A and B: Dynamic and 2D ROESY NMR Study

A. Smirnov,[†] D. B. Fulton,[‡] A. Andreotti,[‡] and J. W. Petrich*,[†]

Contribution from the Department of Chemistry and the Department of Biochemistry, Biophysics and Molecular Biology, Iowa State University, Ames, Iowa 50011

Received February 25, 1999. Revised Manuscript Received June 14, 1999

Abstract: A NMR study was conducted on the antiviral and antitumor agents hypericin and hypocrellin A and B, whose activity is light induced. Elucidation of the conformational/tautomeric properties of these polycyclic quinones is important for interpreting their photophysical behavior in the excited state. Evidence for interconversion between ground-state tautomers or other conformational isomers was sought in temperature-dependent ^{1}H NMR and 2D-ROESY studies. For hypericin and hypocrellin B, only one ground-state species is observed. For hypocrellin A, however, three species are significantly populated in the ground state due to the high flexibility of its 7-membered ring. In the latter case dynamic NMR simulations were performed to obtain kinetic and thermodynamic parameters for the sequential interconversion occurring between the three species. The implications of these results for the interpretation of the light-induced primary processes in these systems are discussed.

1. Introduction

The polycyclic quinones hypericin and hypocrellin (Figure 1) exhibit light-induced antitumor and antiviral activity.[1-4]

Consequently, these compounds have been the subjects of numerous ultrafast and steady-state spectroscopic studies with the goal of elucidating the energetic and dynamic properties of their electronic excited states.[5-24] The corresponding properties of the electronic ground state, though important for interpreting

* To whom correspondence should be addressed.

† Department of Chemistry.

‡ Department of Biochemistry, Biophysics and Molecular Biology.

(1) Duran, N.; Song, P.-S. *Photochem. Photobiol*. **1986**, *43*, 677−680.

(2) Diwu, Z. *Photochem. Photobiol*. **1995**, *61*, 529−539.

(3) Lown, J. W. *Can. J. Chem*. **1997**, *75*, 99−119.

(4) Kraus, G. A.; Zhang, W.; Fehr, M. J.; Petrich, J. W.; Wannemuehler, Y.; Carpenter, S. *Chem. Rev*. **1996**, *96*, 523−535.

(5) Gai, F.; Fehr, M. J.; Petrich, J. W. *J. Phys. Chem*. **1994**, *98*, 5784−5795.

(6) Gai, F.; Fehr, M. J.; Petrich, J. W. *J. Phys. Chem*. **1994**, *98*, 8352−8358.

(7) English, D. S.; Zhang, W.; Kraus, G. A.; Petrich, J. W. *J. Am. Chem. Soc*. **1997**, *119*, 2980−2986.

(8) English, D. S.; Das, K.; Zenner, J. M.; Zhang, W.; Kraus, G. A.; Larock, R. C.; Petrich, J. W. *J. Phys. Chem*. **1997**, *101A*, 3235−3240.

(9) Das, K.; English, D. S.; Fehr, M. J.; Smirnov, A. V.; Petrich, J. W. *J. Phys. Chem*. **1996**, *100*, 18275−18281.

(10) Das, K.; English, D. S.; Petrich, J. W. *J. Am. Chem. Soc*. **1997**, *119*, 2763−2764.

(11) Das, K.; English, D. S.; Petrich, J. W. *J. Phys. Chem*. **1997**, *101A*, 3241−3245.

(12) English, D. S.; Das, K.; Ashby, K. D.; Park, J.; Petrich, J. W.; Castner, E. W., Jr. *J. Am. Chem. Soc*. **1997**, *119*, 11585−11590.

(13) Das, K.; Dertz, E.; Paterson, J.; Zhang, W.; Kraus, G. A.; Petrich, J. W. *J. Phys. Chem. B* **1998**, *102*, 1479−1484.

(14) Fehr, M. J.; McCloskey, M. C.; Petrich, J. W. *J. Am. Chem. Soc*. **1995**, *117*, 1833−1836.

(15) Das, K.; Smirnov, A. V.; Snyder, M. D.; Petrich, J. W. *J. Phys. Chem. B* **1998**, *102*, 6098.

(16) Malkin, J.; Mazur, Y. *Photochem. Photobiol*. **1993**, *57*, 929−933.

(17) Weiner, L.; Mazur, Y. *J. Chem. Soc., Perkin Trans. 2* **1992**, 1439−1442.

(18) Zhang, M.-H.; Weng, M.; Chen, S.; Xia, W.-L.; Jiang, L.-J.; Chen, D.-W. *J. Photochem. Photobiol. A: Chem*. **1996**, *96*, 57.

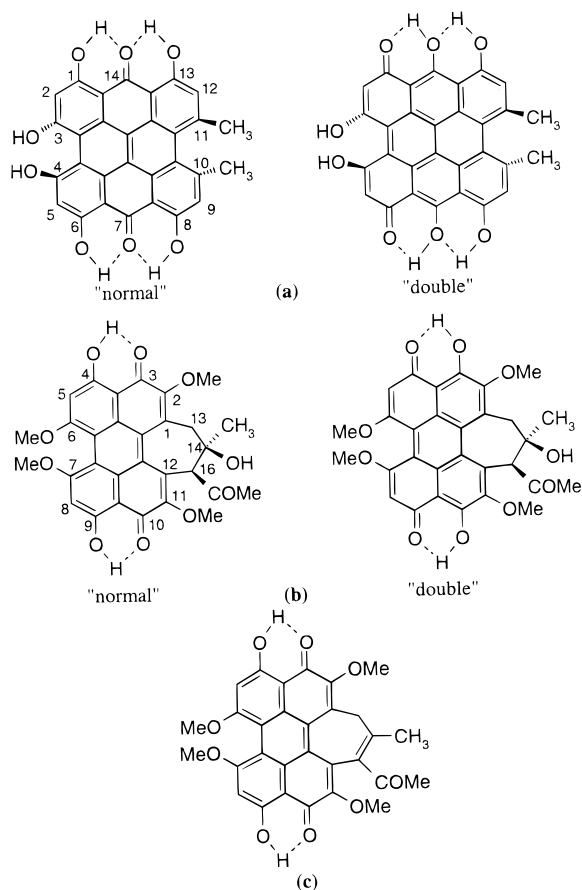(19) Wang, N.; Zhang, Z. *J. Photochem. Photobiol. B: Biol*. **1992**, *14*, 207−217.

Figure 1. Structures of hypericin "normal" and of the "double" tautomer forms (a), hypocrellin A "normal" and "double" tautomer forms (b), and hypocrellin B (c). On the basis of the analogy with hypocrellin A, the form shown for hypocrellin B is the "normal" form.

the photophysical data, have, apart from some exceptions,[27-31] received relatively little attention.

Each of the compounds has a twisted carbon skeleton resulting from the steric strain induced by substituents in the "bay" regions (positions 3, 4 and 10, 11 for hypericin, Figure 1a, and positions 6, 7 and 1, 12 for hypocrellin, Figures 1b and 1c) of the polycyclic ring systems. In addition, for hypocrellin A, the axial chirality arising from such twisting, combined with the chirality of the asymmetric carbon atoms, gives rise to diastereomerism. For some members of the perylenequinone family it has been possible to isolate both diastereomers and to observe their thermal interconversion;[31] but, until now, evidence for interconversion among the hypocrellin A conformers has not been observed.

Hypericin and the hypocrellins are capable of intramolecular hydrogen bond formation so that keto/enol tautomerism is possible. It can be shown through calculations[32,33] and by experimental observation[31] that only certain tautomers are sufficiently stable to be significantly populated at room temperature. For example, in a nonionizing environment hypericin in the ground state is thought to exist as only one tautomer, the so-called normal form[32] (Figure 1a). On the other hand, X-ray[34] and photophysical data[9,15] suggest that hypocrellin A in the ground state exists in at least two tautomeric forms (Figure 1b).

In this article we present an investigation of the ground-state tautomeric and conformational isomers of hypericin and hypocrellin and their temperature-dependent interconversion processes.

2. Experimental Section

Hypericin and hypocrellin A and B were purchased from Molecular Probes, Inc. and used without further purification. ^{1}H NMR spectra were measured in anhydrous DMSO-d_6 and acetone-d_6 (Cambridge Isotope Laboratories) with a Bruker DRX-500 spectrometer. The concentrations were ca. 2 mg cm^{-3}. Chemical shifts are reported relative to 0.05% internal Me$_4$Si. Cross-peaks in 2D ROESY spectra as well as values reported in ref 31 were used in signal assignment. To ensure that there was no concentration dependence associated with the measurements, a series of 1D ^{1}H NMR spectra of hypocrellin A was recorded at 269 K at concentrations from ca. 10^{-5} to 10^{-3} g·cm^{-3}. The number of scans was 64−256, depending on the concentration. The line shapes of spectra at this temperature were in the slow exchange regime. When scaled according to the amount of hypocrellin A in solution, all the signals appeared with chemical shifts, line widths, and intensities that were virtually indistinguishable at different concentrations, and any deviations lay within the uncertainty of the measurements.

1D ^{1}H NMR spectra of hypocrellin A and B were recorded at 293, 298, 308, and 318 K in DMSO and 240, 250, 260, 268, 273, 288, 298, and 313 K in acetone. The line shapes of spectra below 268 K appeared to be in the slow exchange regime. Two-dimensional ROESY data were obtained at 268 K in acetone for two spectral regions: −2.0 to 18.0 and 15.3 to 16.6 ppm.

For hypericin, 1D ^{1}H NMR spectra were recorded at 298, 313, 323, and 333 K in DMSO and 240, 268, 273, 298, and 313 K in acetone. 2D ROESY data were obtained at 298 K in acetone for the spectral range from −2.0 to 18.0 ppm. Hypericin samples were found to decompose upon prolonged exposure to ambient light and were kept in the dark as much as possible.

The 2D-ROESY spectra were acquired at 499.87 MHz with a continuous spin-lock during mixing (RF power 2.5 kHz, mixing time 300 ms) and the carrier frequency set at 8.0 ppm. Typically 340−512 complex FIDs of size 4096 were collected (10 kHz spectral width, relaxation delay 2.0 s, 8 scans/FID) employing the States-TPPI method[38] for phase-sensitive detection in F1. The data were Fourier transformed,

(20) Lu, Y.-Z.; An, J.-Y.; Qin, L.; Jiang, L.-J.; Chiang, L.-C. *J. Photochem. Photobiol. B: Biol.* **1994**, *78*, 247−251.

(21) Yamazaki, T.; Ohta, N.; Yamazaki, I.; Song, P.-S. *J. Phys. Chem.* **1993**, *97*, 7870−7875.

(22) Wells, T. A.; Losi, A.; Dai, R.; Scott, P.; Park, S.-U.; Golbeck, J.; Song, P.-S. *J. Phys. Chem. A* **1997**, *101*, 366−372.

(23) Racinet, H.; Jardon, P.; Gautron, R. *J. Chim. Phys.* **1988**, *85*, 971−977.

(24) Eloy, D.; Pellec, A. Le.; Jardon, P. *J. Chim. Phys.* **1996**, *93*, 442−457.

(25) Darmanyan, A. P.; Burel, L.; Eloy, D.; Jardon, P. *J. Chim. Phys.* **1994**, *91*, 1774−1785.

(26) Angerhofer, A.; Falk, H.; Meyer, J.; Schopel, G. *J. Photochem. Photobiol. B: Biol.* **1993**, *20*, 133−137.

(27) Mikovsky, P.; Sureau, F.; Chinsky, L.; Turpin, P.-Y. *Photochem. Photobiol.* **1995**, *62*, 546−549.

(28) Sanchez-Cortes, S.; Miskovsky, P.; Jancura, D.; Bertoluzza, A. *J. Phys. Chem.* **1996**, *100*, 1938−1944.

(29) Miskovsky, P.; Chinsky, L.; Wheeler, G. V.; Turpin, P.-Y. *J. Biomol. Struct. Dyn.* **1995**, *13*, 547−552.

(30) Miskovsky, P.; Sanchez-Cortes, S.; Jancura, D.; Kocisova, E.; Chinsky, L. *J. Am. Chem. Soc.* **1998**, *120*, 6374−6379.

(31) Arnone, A.; Merlini, L.; Mondelli, R.; Nasini, G.; Ragg, E.; Scaglioni, L.; Weiss, U. *J. Chem. Soc., Perkin Trans. 2* **1993**, 1447−1454.

(32) Petrich, J. W.; Gordon, M. S.; Cagle, M. *J. Phys. Chem. A* **1998**, *102*, 1647−1651.

(33) Etzlstorfer, C.; Falk, H. *Monatsh. Chem.* **1998**, *129*, 855−863.

(34) There is a common assumption in the literature that the most stable form of hypocrellin is that illustrated in Figure 1c. The published X-ray structure indicates C(3)−O(3) and C(10)−O(10) bond lengths that are within experimental error greater than those of their C(4)−O(4) and C(9)−O(9) neighbors.[35] The coordinates available from the Cambridge Crystallographic Data Bank suggest, however, that all four bond lengths are comparable. The former data set is consistent with Figure 1d, enol bonds being longer than keto bonds. The latter data set suggests a mixture of both the normal and the tautomer forms in the ground state. Note that the numbering used in this article differs from that we have employed elsewhere.[8,11]

(35) Wei-shin, C.; Yuan-teng, C.; Xiang-yi, W.; Friedrichs, E.; Puff, H.; Breitmaier, E. *Liebigs Ann. Chem.* **1981**, 1880−1885.

(36) Freeman, D.; Frolow, F.; Kapinus, E.; Lavie, D.; Lavie, G.; Meruelo, D.; Mazur, Y. *J. Chem. Soc., Chem. Commun.* **1994**, 891.

Table 1. ¹H Chemical Shift Values (δ, ppm) for Hypericin and Hypocrellin A and B at 298 K

compd	hypericin acetone	hypericin DMSO	hypocrellin A acetone	hypocrellin B acetone
phenolic hydroxyls	14.82 (8,13-OH) 14.27 (1,6-OH)	14.74 (8,13-OH) 14.09 (1,6-OH)	16.05−16.45[a]	16.34, 16.37[c]
aromatic hydrogens	7.35 (9,12-H) 6.62 (2,5-H)	7.46 (9,12-H), 6.59 (2,5-H)	6.76 (b) (5,8-H)	16.58, 16.60[c] (5,8-H)
methoxy			4.07, 4.14, 4.21 (b)[c]	4.04, 4.16, 4.19, 4.20[c]
methylene			3.4−3.75; 2.4−2.8[b]	4.07 (d, 13-H$_a$), 4.34 (d, 13-H$_b$)
methyne			3.84, 4.79, 5.78 (all for 16-H)	
methyl	2.78	2.75	1.6−1.7 (15-H$_3$), 1.89 (18-H$_3$)	1.81 (18-H$_3$), 2.35 (15-H$_3$)

[a] See Table 3 for detailed assignment. [b] See Table 2 for detailed assignment. [c] Detailed assignment was not possible or attempted.

zero-filled, and apodized with a 90° shifted sine-bell squared function to yield 4096 × 512 real data points. The baseline of the 2D spectrum was corrected in both dimensions with a fifth degree polynomial fitting algorithm. In the second hypocrellin ROESY experiment (over a spectral range of 15.3−16.6 ppm) offset and sweep width were adjusted to obtain a high-resolution spectrum of the downfield hydroxyl region. The spin-lock frequency was set upfield from the region of interest to avoid coherent (TOCSY-type) transfer artifacts.[39]

Dynamic NMR simulations were performed with the program XNMR written by Uwe Seimet, Germany (available at ftp://acp5.chemie. uni-kl.de/pub/xnmr), and Mex written by Alex Bain, McMaster University (for information see http://www.chemistry.mcmaster.ca/ faculty/bain). The two simulation programs produced identical results. The spectrum at 240 K was treated as having a zero interconversion rate for every pair of species. This was necessary to estimate chemical shifts and line widths at the slow exchange limit, which were fixed parameters in the simulations.

3. Results and Discussion

A. Hypericin. The aromatic skeleton of hypericin adopts a nonplanar, twisted geometry due to the steric repulsion between the two methyl groups. This geometry retains a C_2 symmetry axis and magnetic equivalence of the corresponding protons in the upper and the lower part of the molecule (Figure 1a), resulting in a rather simple NMR spectrum. However, analysis of the NMR data was complicated by the presence of impurities in the commercially available material. The signals from impurities, water and the partially deuterated solvent molecules, were discriminated on the basis of their relative integrals and the expected values of their chemical shifts.

The ¹H NMR signals were assigned mostly based on the values of the chemical shifts (Table 1). We note that two methyl resonances were shifted considerably to the low field (2.75 ppm) as a consequence of anisotropic deshielding by the polyaromatic system in combination with the significant steric hindrance.

The primary goal of our NMR study of hypericin was to obtain experimental verification of the species populating the hypericin ground state, which may consist of at least six nonionized tautomeric species:[32] the normal form (Figure 1a); two monotautomers, arising from the transfer of one proton; and three double tautomers (e.g., Figure 1b), arising from the transfer of a proton at the "top" and the "bottom" of the molecule. One of these double tautomers, in which the proton is transferred from opposite sides of the molecule, does *not* correspond to a minimum on the potential energy surface.[32]

(37) Etzlstorfer, C.; Falk, H.; Müller, N.; Schmitzberger, W.; Wagner, U. G. *Monatsh. Chem.* **1993**, *124*, 751−761. (b) Falk, H. Personal communication.

(38) Marion, D.; Ikura, M.; Tschudin, R.; Bax, A. *J. Magn. Reson.* **1989**, *85*, 393.

(39) (a) Hennig, J.; Limbach, H. H. *J. Magn. Reson.,* **1982**, *49*, 322. (b) Bax, A.; Davis, D. G. *J. Magn. Reson.* **1985**, *63*, 207.
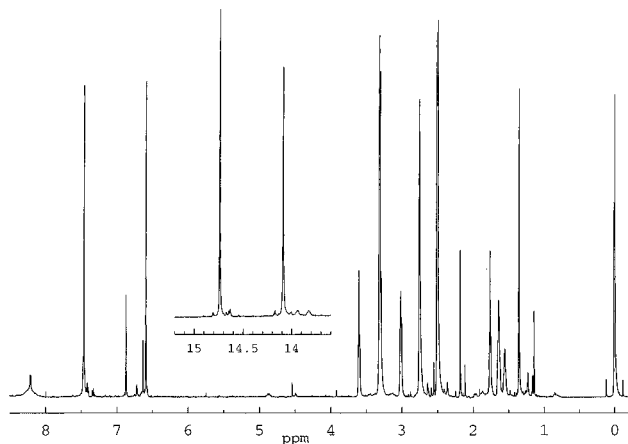

Figure 2. 1D ¹H NMR spectrum of hypericin in DMSO at 298 K. No line shape coalescence typical of an exchanging system was observed but sample exhibited temperature-dependent line narrowing. As is evident from the low-temperature data, this line narrowing clearly comes from lower viscosity of DMSO at higher temperatures and not due to the increased interconversion rate among possible tautomers. In the latter case, we would expect substantial signal broadening or even peak splitting at low temperatures.

We collected ¹H NMR spectra in the temperature range from 240 to 333 K in DMSO and acetone, solvents of different viscosity and polarity. Our attention was directed to the aromatic and very low-field (13−14 ppm) regions of the spectra where tautomerization processes are expected to be the most evident. In the aromatic region of the spectrum we observed two strong singlets at 6.6 and 7.4 ppm each flanked by a number of weaker satellites (Figure 2). In DMSO over the temperature range 298− 333 K no line shape coalescence typical of an exchanging system was observed. The temperature dependence of the satellite chemical shifts appeared to be either negligible or about an order of magnitude greater than that of the main components (from 6.63 ppm at 298 K to 6.40 ppm at 333 K). In addition, a small peak emerged from the shoulder of the aromatic hydrogen signal at 7.4 ppm, shifting to lower field as the temperature increased. By carefully overlaying and comparing the data obtained at various temperatures for this spectral region we concluded that the observed changes in the NMR spectra were due to impurities and to the temperature dependence of the chemical shifts and line widths of hypericin aromatic signals. We conclude that this line narrowing arises from the lower viscosity of DMSO at higher temperatures and not from an increased interconversion rate among possible tautomers. Consistent with this conclusion is that as the temperature is lowered to just above the freezing point of DMSO, and even lower (240 K) in acetone, no substantial increase in the line broadening of either aromatic or *peri*-hydroxyl signals was observed.
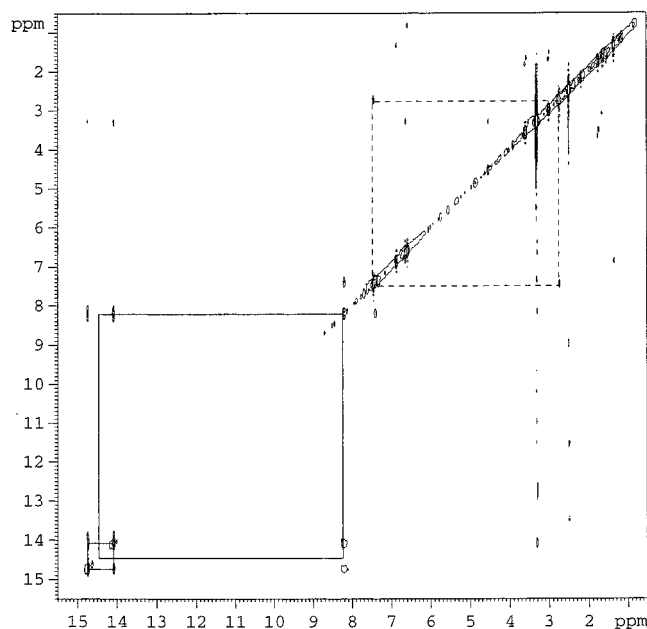
Figure 3. 2D ROESY spectrum of hypericin in DMSO at 298 K. Solid lines denote positive contours; dashed lines denote negative contours.

Hypericin possesses three pairs of nonequivalent phenolic hydroxyls in its most stable tautomeric form, the "normal" form (Figure 1a). In DMSO, the ^{1}H NMR signal of the bay hydroxyls was observed as a broad line in the expected region (8.1–8.3 ppm) that shifted slightly to higher field as the temperature increased. On the other hand, another pair of relatively narrow lines were observed at very low field (14.08 and 14.73 ppm at 298 K) and exhibited almost no chemical shift temperature dependence, attributes indicative of intramolecular hydrogen bonding.[40] These lines were assigned to the *peri*-hydroxyls (positions 1, 6, 8, and 13 (Figure 1a)).

We conclude that the ground state of hypericin at temperatures as high as 333 K is represented by a single tautomer. Based on the X-ray data[36,37] and the results of ab initio quantum mechanical calculations,[32] the structure of this tautomer is given by Figure 1a. As will be shown below, this is in contrast to what is observed for hypocrellin A.

To assist in the assignment of the low-field phenolic and aromatic signals of hypericin, a 2D ROESY (rotating-frame Overhauser enhancement spectroscopy) NMR spectrum[39,41,42] was acquired in DMSO at 298 K (Figure 3). The ROESY experiment has two advantages over NOESY[43] for this study: the magnitude of rotating-frame cross-relaxation is favorable for molecules of this size, and ROE cross-peaks are readily distinguished from chemical exchange or *J*-correlated cross-peaks by their negative phase relative to the diagonal signals. Both positive- and negative-phase signals can be observed in the ROE experiment. In the absence of TOCSY and HOHAHA artifacts, positive-phase signals indicate a chemical or a conformational exchange process in which the proton changes its chemical shift (i.e., its environment). Negative-phase signals arise from the interactions of protons, in close proximity, within the molecule (i.e., the same conformational or tautomeric species).

The aromatic signal at 7.4 ppm (assigned to 9-H and 12-H) is correlated to the methyl singlet at 2.75 ppm via an intense negative ROE cross-peak, whereas its neighbor at 6.6 ppm (2-H and 5-H) has no cross-peaks at all (Figure 3). Due to their proximity to the bay hydroxyl groups, protons 9-H and 12-H are deshielded relative to protons 2-H and 5-H. This is because hydroxyl groups are much stronger π-donors than methyl groups.

It is more difficult to assign the nonequivalent intramolecular hydrogen-bonding hydroxyls (in the 14–15 ppm region) since neither of these signals has negative cross-peaks with the aromatic or methyl hydrogens.

Although DMSO bears no labile hydrogens, significant hydrogen chemical exchange among all three types of hydroxyls was evident from positive cross-peaks in the ROESY spectrum. If we assume that this exchange, although perhaps mediated by traces of water in the solvent, is intramolecular, then it is reasonable to expect that the proton exchange rate among hydroxyls in close proximity will be greater than for those that are further apart. Hence, positive cross-peaks in the ROESY spectrum should have a higher volume for correlation between 1-OH and 3-OH (and, by symmetry, 6-OH and 4-OH) as compared to 13-OH and 3-OH (and, by symmetry, 8-OH and 4-OH). Based on this consideration, the peak at 14.08 ppm can be assigned to 1-OH and 6-OH and that at 14.73 ppm to 8-OH and 13-OH.

B. Hypocrellin A. i. Ground-State Conformational Isomers. The room-temperature ^{1}H NMR spectrum of hypocrellin A in acetone is almost identical to that which has been previously reported.[31] However, we observe that lowering the temperature to 268 K results in significant changes and increased spectral complexity, especially in the low- and medium-field spectral regions. Similar changes were observed at low temperature in DMSO but with considerably broader lines. As in the case of hypericin, the analysis was slightly complicated by the presence of impurities, the most abundant of which is hypocrellin B. By changing temperatures and by using 2D ROESY, most of these ambiguities were, however, successfully resolved.

The ^{1}H NMR spectrum of hypocrellin A is more complex than that of hypericin because of its lower symmetry and, as will be seen, the interconversion between conformational isomers and tautomeric forms. The presence of two asymmetric centers (C-16 and C-14), in combination with the helical topology of the aromatic ring system, permits hypocrellin to exist in two possible forms, denoted gauche and anti in Figure 4. The two conformers differ principally in the configuration of the invertible seven-membered ring fragment. The acetyl group attached to C-16 is expected to be sterically restricted in its rotation about the C(16)–C(17) σ-bond, especially at low temperature. If the interconversion among the conformers is slow on the NMR time scale, peak broadening or even splitting will be observed due to differential anisotropic deshielding by the aromatic ring system and by the restricted acetyl's carbonyl group. In addition, each of the conformers can undergo keto–enol type tautomerization (Figure 1b). Tautomeric interconversion will affect the hydroxyl NMR signals directly, and may indirectly perturb the chemical shifts of other protons via changes in the conjugation of the polycyclic ring system.

We observed nonequivalence of the aromatic and hydroxy protons despite the large distance to the acetyl group, which acts as the asymmetry-inducing moiety. Several peaks show additional splittings due to conformer/tautomer interconversion
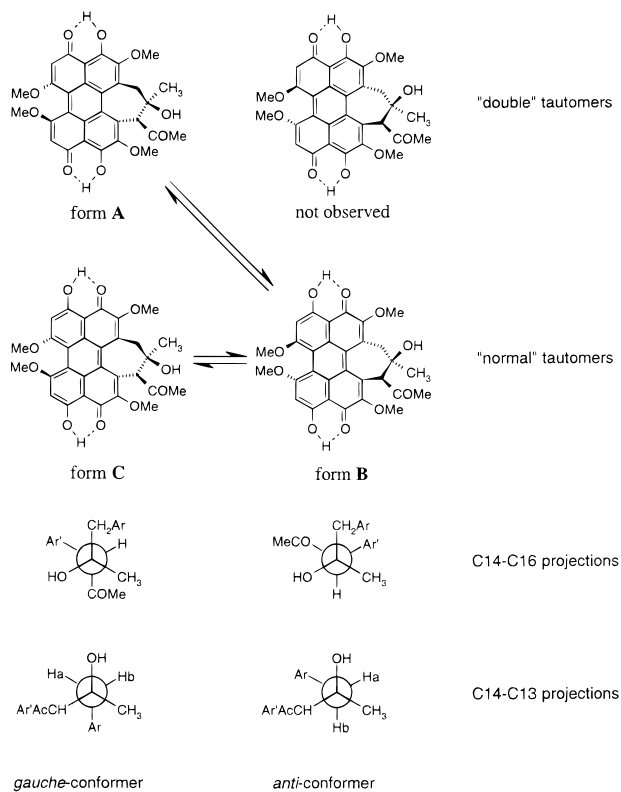
(40) Schaefer, T. *J. Phys. Chem.* **1975**, *17*, 1888.
(41) Bothner-By, A. A.; Stephens, R. L.; Lee, J. M.; Warren, C. D.; Jeanloz, R. W. *J. Am. Chem. Soc.* **1984**, *106*, 811.
(42) Bax, A.; Grzesick, S. In *Encyclopedia of Nuclear Magnetic Resonance*; Grant, D. M., Harris, R. K., Eds.: Wiley: New York, 1996; pp 4157–4167.
(43) Jeener, J.; Meier, B. H.; Bachman, P.; Ernst, R. R. *J. Chem. Phys.* **1979**, *71*, 4546.

Figure 4. Possible conformational forms of the hypocrellin A normal and double tautomers. The anti/gauche nomenclature is based on the relative position of the methyl and acetyl moieties as depicted by the C(13)−C(16) Newman projection. Only species **A**, **B**, and **C** are present at room temperature as is apparent from 2D ROESY NMR spectra (see Figure 6).
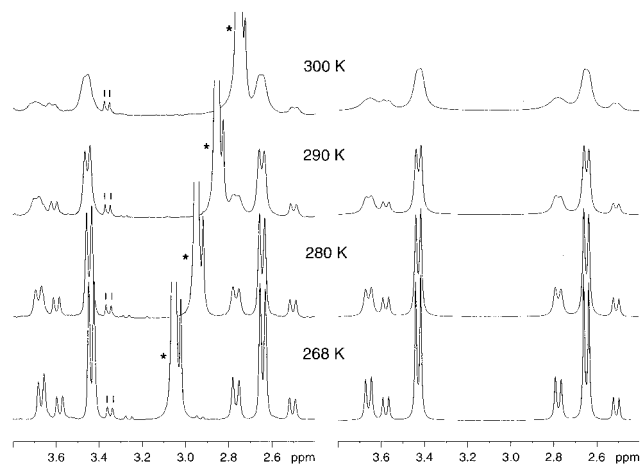

Figure 5. Dynamic NMR spectra of hypocrellin A doublets as a function of temperature. Experimental and simulated data are presented respectively on the left and right. Asterisks denote impurities, and small vertical dashes denote signals from hypocrellin B.

processes, as is evident in the temperature-dependent and ROESY data.

In spectra recorded in acetone at 268 K, we observe a group of six doublets in the aliphatic region each with an identical geminal coupling constant but with differing intensities (Figure 5). Among this group are three pairs of doublets, each of comparable intensity, that are correlated by negative ROESY cross-peaks (Figure 6). These pairs of doublets are attributed to the methylene group (13-H$_a$ and 13-H$_b$, Figure 4) of the seven-membered ring appearing at different chemical shifts due to slow interconversion among multiple conformations. The rela-
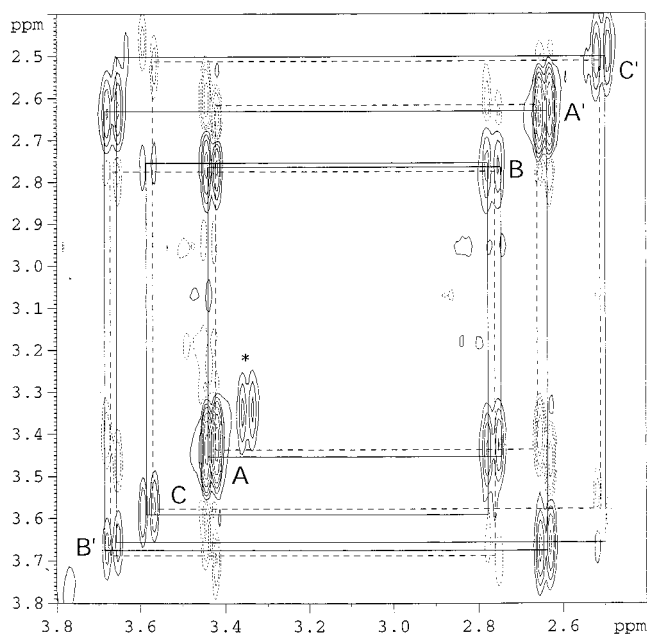

Figure 6. 2D ROESY NMR spectrum of hypocrellin A methylene H$_a$ (**A**, **B**, **C**) and H$_b$ (**A′**, **B′**, **C′**) protons at 268 K. Solid lines denote positive contours; dashed lines denote negative contours. An asterisk (*) denotes peaks due to the traces of hypocrellin B. Water peaks have been removed to clarify the spectrum.

tionship among these signals is revealed by exchange (positive) ROESY cross-peaks. The two strongest doublets (centered at 3.43 and 2.65 ppm) of similar intensity have exchange correlations to two weaker ones (centered at 2.75 and 3.65 ppm, respectively). In addition, the latter doublet has another pair of exchange correlations to doublets centered at 3.60 and 2.50 ppm, respectively, which are of intermediate intensity among the three pairs. *In the ground state, three significantly populated conformational species (**A**, **B**, and **C**) are therefore involved in an interconversion process (**A** ⇌ **B** ⇌ **C**) in which there is no appreciable interconversion between species **A** and **C**.* At 300 K, the ground-state population is 60.6% **A**, 29.4% **B**, and 10% **C**.

A similar three-site exchange pattern is observed involving singlets at 3.8 (**A**), 4.8 (**B**), and 5.8 (**C**) ppm, and is assigned to the methyne proton 16-H (Figure 7). Their relative intensities, however, only qualitatively follow the same pattern as for the 13-H doublets: accurate intensity measurements in this region of the spectrum were difficult due to overlapping signals from impurities.

In a separate ROESY experiment with a spectral window covering the low-field (hydroxyl) part of the spectrum (Figures 8 and 9) we observed strong positive cross-peaks between pairs of singlets at 16.12, 16.20 ppm (**A**) and 16.48, 16.40 ppm (**B**), respectively as well as between the latter singlets and a pair at 16.13, 16.04 ppm (C, which partially overlaps peak **A**), again indicating an exchanging system of type **A** ⇌ **B** ⇌ C. The order of the labels **A**, **B**, and **C** relative to the 13-H methylenes was deduced from the relative intensities of the peaks.

As further evidence of interconversion between conformers, a multiplet at about 6.8 ppm (due to aromatic protons 2-H and 5-H) coalesces to the broadened singlet as the temperature is raised to 313 K. This multiplet has negative cross-peaks to another strong multiplet at 4.2 ppm due to the nearby methoxy protons. (Figure 7).

The 15-H methyl and 18-H (acetyl) methyl peaks also exhibit evidence of conformational exchange. Each methyl is observed
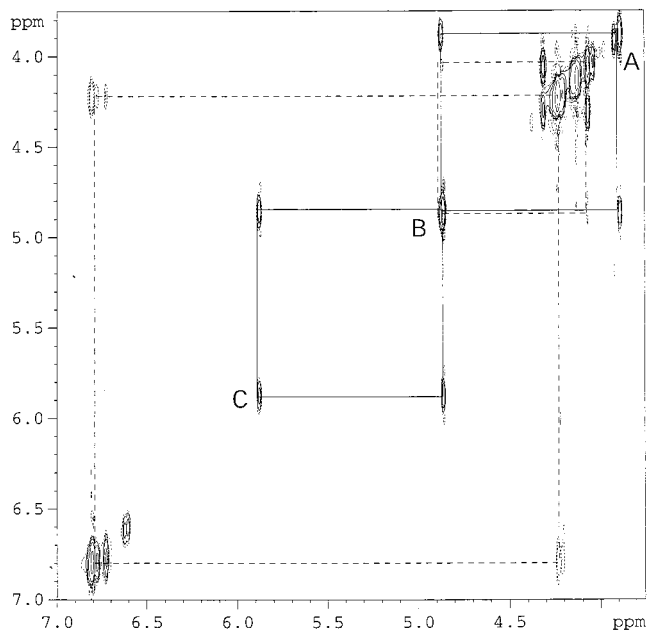
Figure 7. 2D ROESY NMR spectrum of hypocrellin A aromatic and methyne protons. Solid lines denote positive contours; dashed lines denote negative contours. Water peaks have been removed to clarify the spectrum.
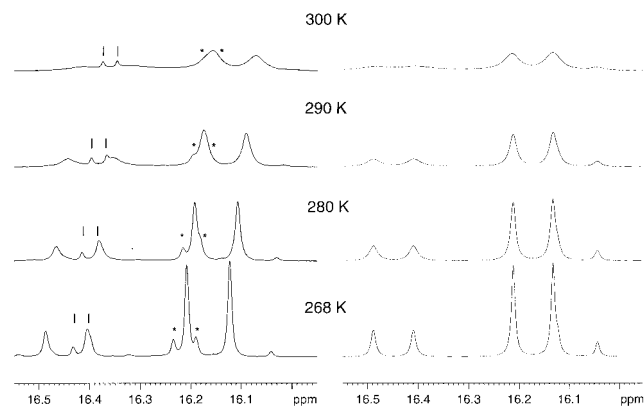

Figure 9. 2D ROESY NMR spectrum of hypocrellin A in the low-field region at 268 K, showing signals from phenolic hydroxyls. Only positive-phase cross-peaks (arising from tautomeric exchange) are evident in this region. Water peaks have been removed to clarify the spectrum.

Figure 8. Dynamic NMR spectra hypocrellin A low-field region as a function of temperature. Experimental and simulated data are presented respectively on the left and right. Asterisks denote impurities, and small vertical dashes denote signals from hypocrellin B. Due to the numerous factors that can affect line shapes of hydrogen-bonded protons it was only possible to achieve qualitative agreement with the experimental spectrum and be consistent with simulations for the aliphatic region (see Figure 5). Asterisks denote impurities, and small vertical dashes denote hypocrellin B.

Figure 10. 2D ROESY NMR spectrum of hypocrellin A in the high-field region at 268 K showing signals of 15-H and 18-H methyls. Solid lines denote positive contours, whereas dashed lines denote negative contours. Water peaks have been removed to clarify the spectrum.

at two chemical shifts (1.5 and 1.6 ppm for 15-H, and 1.9 and 1.3 ppm for 18-H) correlated by positive cross-peaks (Figure 10). In both cases, the downfield peak had much greater intensity. The observation of distinct conformational species for the acetyl methyl confirms that its position is sterically hindered.

Having a general picture of the dynamic equilibrium of this system, we now describe the specific conformers corresponding to species **A**, **B,** and **C**. The cross-peak pattern in the ROESY data shows that the chemical shift order of the 13-H_a and 13-H_b methylene doublets is reversed upon conversion from the **A** to the **B** species, and is again reversed on conversion to the **C** species (Figure 6). Inspection of Figure 4 shows that protons 13-H_a and 13-H_b interchange their lateral distance to the polycyclic ring system and to the acetyl group (denoted as Ar′Ac) on conversion between the gauche and anti diastereo-
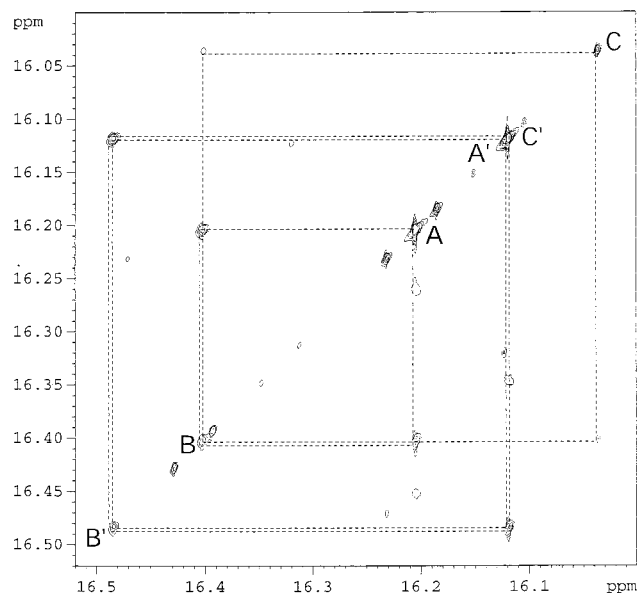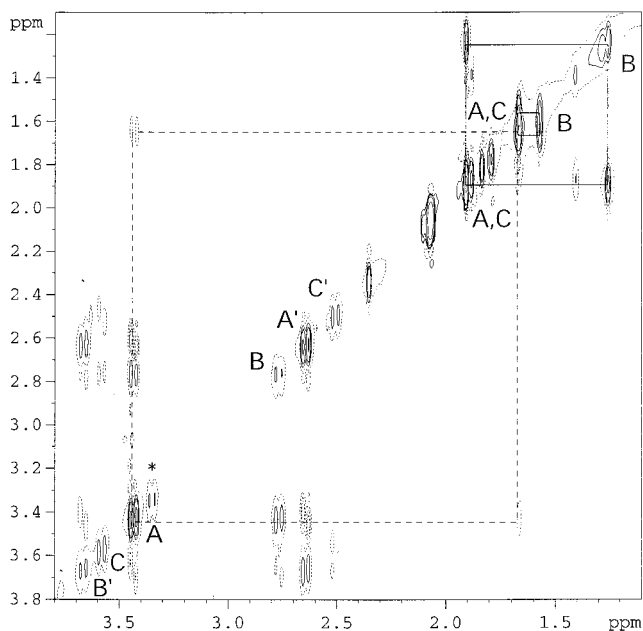
mers. It is reasonable to expect that the component of the chemical shifts of the doublets due to anisotropic deshielding will also be reversed in the gauche and anti forms. Hence, we conclude that each step in the sequence **A** ⇌ **B** ⇌ **C** includes a gauche−anti conformational change. Next, we note that in the gauche form the methyl group attached to C-15 is in the anti position to 13-H_b whereas in the anti form it is equidistant to both 13-H_a and 13-H_b (Figure 4). A negative cross-peak to the methyl signal at 1.7 ppm is observed for only one of the doublets of species **A** (centered at 3.43 ppm) (see Figure 10). We conclude that species **A** and **C** are gauche conformers, **B** is an anti conformer, and the geminal doublets may be stereospecifically assigned as given in Table 2.

Table 2. Chemical Shift of Hypocrellin A Doublets in NMR Spectrum and Assignment of Conformer Type for Species **A**, **B**, and **C**

	doublet center shift, ppm		methyne	conformer
species	H_a	H_b	shift, ppm	type
A	3.43	2.65	3.8	gauche
B	2.75	3.65	4.8	anti
C	3.60	2.50	5.8	gauche

ii. Ground-State Tautomers. Referring now to the hydroxyl region of the spectrum, a change in chemical shift order was observed between species **A** and **B** but not between **B** and **C** (see Figure 9 and Table 2). Given the distance from the flexible portion of the seven-membered ring to the hydroxyls, it is unlikely that the anti/gauche diastereomerism is influencing these shifts. Rather, the dominating factor is expected to be hydrogen bond strength, i.e., the tautomeric state. Therefore it is likely that during the first (but not the second) conversion step in the **A** ⇌ **B** ⇌ C system, there is a change in tautomeric state accompanied by a change in the aromatic structure (conjugation) of the polycyclic system. This would explain the change in the order of chemical shifts of exchanging hydroxyls and the deshielding of methylene protons 13-$H_{a,b}$ and methyne proton 16-H in **B** as compared to **A** (Figure 8).

Based on the observation from X-ray crystallography[35] that the double tautomer of hypocrellin is the form isolated, we propose that the most populated form (**A**) of hypocrellin is the gauche diastereomer of the "double" tautomer. The anti diastereomer of the "double" tautomer is apparently not sufficiently populated to be observed under our experimental conditions. This is plausible since such a species would be destabilized by the π-bond and acetyl oxygen lone pair interactions, and would undergo rapid double-proton transfer to the "normal" tautomer (**B**).

These conclusions are also consistent with the observation of only two exchanging species for the 15-H and 18-H methyls (Figure 10), since their shifts are not expected to be influenced by the tautomeric state, i.e., states **A** and **C** (both in the gauche conformation) are indistinguishable with respect to the methyls. The relative ground-state populations are thus as follows: 60.6% **A** (gauche double tautomer), 29.4% **B** (anti normal tautomer), and 10% **C** (gauche normal tautomer).

iii. Simulating the Proposed Model for Hypocrellin A. To validate our model of interconverting tautomers/conformers we performed dynamic NMR simulations of hypocrellin A spectra in the temperature range from 268 to 300 K. In performing these simulations, we assumed that the NMR line widths (in the absence of exchange broadening), the enthalpy and entropy of reaction, and the activation enthalpy and entropy all had negligible temperature dependence. A temperature-independent line width corresponding to an effective relaxation time T_2^* equal to 0.08 s was assumed for each type of proton. *This value is derived from the low-temperature line widths that experimentally proved to have no temperature dependence in the range from 240 to 260 K.* In addition, it was assumed that the interconversion rates at 240 K were negligible, and the chemical shifts at this temperature were taken to be the slow exchange-limited values. Our simulations did not account for the relative differences in temperature dependence of resonance frequencies for the protons involved. We believe this to be a reasonable assumption as the exchange processes studied occur among the hydrogen atoms of similar chemical environments. The relative population of species **A**, **B**, and **C** at each temperature above 268 K had to be estimated because the spectra at these

temperatures had intermediate-exchange line shapes and could not be reliably integrated. This was done by extrapolation of the equilibrium constant to higher temperatures, once $\Delta H°$ and $\Delta S°$ for each process had been calculated by linear regression analysis from the van't Hoff equation

$$\ln K = -\Delta G°/RT = -\Delta H°/RT + \Delta S°/R$$

The equilibrium constants K at temperatures 240, 250, 260, and 268 K were obtained from ratios of the integrals of methylene signals in the 2.45−2.90 ppm range, where interference with water and other impurities is minimal (Table 4).

While the relative populations of **A**, **B**, and **C** were held fixed at the calculated values, the interconversion rates from **A** to **B** and from **B** to **C** where allowed to vary until qualitative agreement between simulated and experimental line shape was achieved for each temperature (Figure 5). The same set of parameters was used to simulate data for the phenolic hydroxyl and methylene spectral regions (Figures 5 and 8). The activation enthalpy $\Delta H^‡$ and entropy $\Delta S^‡$ (Table 4) were recovered from the Eyring equation

$$k = \kappa k_B T \exp(-\Delta G^‡/RT)/h$$

or

$$\ln(k/T) = 23.76 - (\Delta H^‡/RT) + (\Delta S^‡/R)$$

where κ is the transmission coefficient, which is equal to unity if every transition state decays to product. The latter equation allowed for simple linear least-squares analysis illustrated in Figure 13. (We use the Eyring equation because it allows extraction of activation parameters that are temperature independent. Fitting the data to a simple Arrhenius law with a temperature-independent prefactor also produces a straight line within experimental error.)

Our model involves three species **A**, **B**, and **C**, which sequentially interconvert among each other as represented by the following equation:

$$A \underset{k_{-1}}{\overset{k_1}{\rightleftarrows}} B \underset{k_{-2}}{\overset{k_2}{\rightleftarrows}} C$$
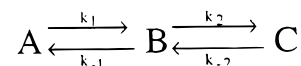
Forward and reverse rate constant are related to the reaction equilibrium constant as given by

$$K_{AB} = [\mathbf{B}]/[\mathbf{A}] = k_1/k_{-1} \qquad K_{BC} = [\mathbf{C}]/[\mathbf{B}] = k_2/k_{-2}$$

where [**A**], [**B**], and [**C**] are populations of species **A**, **B**, and **C** respectively. There is no interconversion between **A** and **C** in this model because we do not observe any positive cross-peaks for their signals in the 2D ROESY NMR spectra. Consistent with our assignments of states **A**, **B**, and **C** is the observation that the activation enthalpy for the **B** → **A** process is greater than that for the **B** → **C** process. This is because **B** → **A** involves both tautomerization and a conformational transition of the carbon skeleton, whereas **B** → **C** only involves the gauche−anti transition.

C. Hypocrellin B. Hypocrellin B (Figure 1c) is very similar in structure to hypocrellin A and accompanies it in natural and commercial products.[44,45] Hypocrellin B is formed by the elimination of a water molecule at the C-14 and C-16 positions

(44) Kishi, T.; Tahara, S.; Taniguchi, N.; Tsuda, M.; Tanaka, C.; Takahashi, S. *Planta Med.* **1991**, *57*, 376−379.

(45) Wang, N.; Zhang, Z. *J. Photochem. Photobiol. B* **1992**, *14*, 207−217.

Table 3. Chemical Shifts of Hypocrellin A Peri-Hydroxyls in the NMR Spectrum and Assignment of Tautomer Type for Species **A**, **B**, and **C**

species	hydroxyl shift, ppm		tautomer type[a]
	OH	OH′	
A	16.12	16.20	double
B	16.48	16.40	normal
C	16.13[b]	16.04	normal

[a] The exact assignment of structure for **A** (double or normal) and other species respectively still needs further evidence such as energy calculation in crystal and in solution or high-quality theoretical estimation of chemical shifts of peri-hydroxyls. [b] This signal is assumed to overlap with the one originating from species **A**.

of hypocrellin A to form a C−C double bond in the seven-membered ring. We anticipate that this double bond restricts rotation around the C(14)−C(16) bond and hence restricts interconversion between conformers, in contrast to hypocrellin A. The formation of the double bond also removes both chiral centers (at C14 and C16). However, the double bond does not render the molecule planar, and two conformational isomers differing in the sense of twist of the perylenequinone skeleton can still coexist. In contrast to hypocrellin A, however, the two atropoisomers constitute an enantiomeric pair and thus are energetically equivalent. This by no means implies that 13-H_a and 13-H_b are no longer diastereotopic, but suggests that they will interchange chemical shift should there be interconversion of conformers.

Hypocrellin B can exist in two stable tautomeric forms, analogous to the normal and double tautomers of hypocrellin A. There is a possible resonance interaction of the C(14)−C(16) double bond with the aromatic π-system despite the significant torsion angle relative to the molecular plane. Such an interaction should result in a significant difference in energy for the two tautomers, and we expect to observe only one dominating species in the ground-state population of hypocrellin B at room temperature and below.

As anticipated, the ^{1}H NMR spectrum of hypocrellin B in acetone is much simpler than that of hypocrellin A (Figure 11). Lowering the temperature from 313 to 240 K did not have a significant effect, except for the signals due to phenolic protons at 16.2−16.5 ppm. At low temperature, this region showed two pairs of singlets with significantly different relative intensities (Figure 12). Each pair was assigned to the nonequivalent aromatic hydrogens at the C-5 and C-7 positions. As the temperature is increased from 268 to 313K, the lines gradually broaden due to the proton-exchange processes and the weaker pair of singlets coalesces with the dominant one. (This is in contrast to the pair of nonequivalent aliphatic protons, which we referred to as 13-H_a and 13-H_b for hypocrellin A.) Having a typical geminal coupling constant of 11.6 Hz, their line shapes are only slightly broadened at 313 K (Figure 11). This indicates that, in contrast to hypocrellin A, interconversion between two possible atropoisomers of hypocrellin B is largely impeded at room temperature. A consequence of this latter observation should be the possibility of isolating (+) and (−) forms, which absorb circularly polarized light differently. However, the only report of which we are aware[44] states that the isolated natural product was not found optically active.

Consistent with the dynamic NMR experiments, the 2D ROESY spectrum of hypocrellin B exhibited only negative cross-peaks (Figure 12). The expected exchange cross-peaks among phenolic hydroxyls could not be observed due to the limited spectral resolution, large difference in intensity, and significant overlap of the singlet pairs. As in the case of

hypocrellin A we observed significant ROE between aromatic (6.6 ppm) and methoxy (4.2 ppm), geminal H_a and H_b protons (4.1 and 3.3 ppm), and to a smaller extent between one of the geminal (4.1 ppm) and methyl (1.8 ppm) hydrogens. A negative cross-peak between acetyl (2.35 ppm) and a signal at about 4.1 ppm could not be resolved with confidence but most likely is due to the proximity of the methoxy group at the C-11 position.

Both 2D ROESY and 1D dynamic NMR data lead to the conclusion that due to the double bond in the seven-member ring, hypocrellin B has higher structural rigidity than hypocrellin A. Consequently, only one tautomer of hypocrellin B is significantly populated in the ground state.

4. Conclusions

Based on the results of the present NMR study it appears that hypericin in DMSO or acetone exists as a single conformer/tautomer even at temperatures as high as 333 K (or at least that multiple conformers or tautomers cannot be detected by means of NMR spectroscopy). Its aromatic signals are now unambiguously assigned and interpreted. Proton exchange among all of the three pairs of hydroxyls was observed on the time scale of <300 ms.

Hypocrellin A was shown to exist in an equilibrium involving three significantly populated species with an interconversion scheme that can be represented schematically as **A** ⇌ **B** ⇌ **C**. Based on the detailed analysis of its 2D ROESY spectrum in acetone at 268 K, it was deduced that the most populated species, **A**, is most likely the ***double*** tautomer in the gauche conformation; the least populated species, **B**, is the ***normal*** tautomer in the anti conformation; and **C** is the ***normal*** tautomer in the gauche form. Both interconversion barriers are small enough to be frequently crossed on the time scale of the NMR experiment at temperatures of 298 K and above. (It is important to stress that the assignments regarding the *tautomeric* forms of **A**, **B**, and **C** are tentative and arise only from chemical shift arguments and X-ray data. On the other hand, the *conformational* assignment of gauche or anti is believed to be determined to a high degree of certainty.)

In contrast to hypocrellin A, its dehydrated form hypocrellin B exhibits less complex spectra that are believed to arise from a single dominant species stabilized by the double bond in the seven-membered ring.

The results of this NMR study are important for understanding the photophysics of hypericin and hypocrellin. The assignment of the primary photoprocess in hypericin and hypocrellin has now been unambiguously attributed to excited-state intramolecular atom transfer by means of transient absorption and fluorescence upconversion experiments and a careful comparison of the kinetics of methoxy analogues incapable of executing such processes. When this assignment was proposed in our early studies of hypericin, it was not, however, readily accepted in part because of the mirror image symmetry existing between the absorption and emission spectra. Such symmetry is typically taken as a signature of negligible structural changes between the absorbing and the emitting species. Intramolecular excited-state proton transfer usually generates a broad structureless emission spectrum that bears little resemblance to the absorbance spectrum. 3-Hydroxyflavone provides a good example.[46−49]

(46) Schwartz, B. J.; Peteanu, L. A.; Harris, C. B. *J. Phys. Chem.* **1992**, *96*, 3591−3598.
(47) Brucker, G. A.; Swinney, T. C.; Kelley, D. F. *J. Phys. Chem.* **1991**, *95*, 3190−3195.
(48) Strandjord, A. J. G.; Barbara, P. F. *J. Phys. Chem.* **1985**, *89*, 2355−2361.
(49) McMorrow, D.; Kasha, M. *J. Phys. Chem.* **1984**, *88*, 2235−2243.

Table 4. Simulation Results of Hypocrellin A Dynamic NMR Spectra Based on the Model of Three Interconverting Species **A**, **B**, and **C**

process	equil constant at 300 K	$\Delta H°$, kJ/mol	$\Delta S°$, J/(mol K)	$\Delta G°$, kJ/mol	interconversion rate[a] at 300 K, s^{-1}	$\Delta H^{\ddagger}$, kJ/mol	$\Delta S^{\ddagger}$, J/(mol K)	$\Delta G^{\ddagger}$, kJ/mol
A → B	0.49	5.5 ± 0.3	12 ± 1	1.9	45	67 ± 4	10 ± 12	64.0
B → A	2.05	-5.5 ± 0.3	-12 ± 1	-1.9	93	62 ± 4	-3 ± 10	62.9
B → C	0.34	-6.5 ± 0.5	-31 ± 2	2.7	20	51 ± 2	-55 ± 7	67.4
C → B	2.95	6.5 ± 0.5	31 ± 2	-2.7	43	57 ± 2	-26 ± 7	64.7

[a] These values are based on the *assumption* that the transverse relaxation time T_2^* is temperature independent and interconversion exchange rates are negligible at 240 K. Our measurements indicate that the line widths have no temperature dependence in the range from 240 to 260 K. Quantitative 1D or 2D ROESY experiments as a function of mixing time would be needed to obtain exact rate constants since the line shapes yield $1/T_2^* + k_{AB}$ or $1/T_2^* + k_{BC}$.
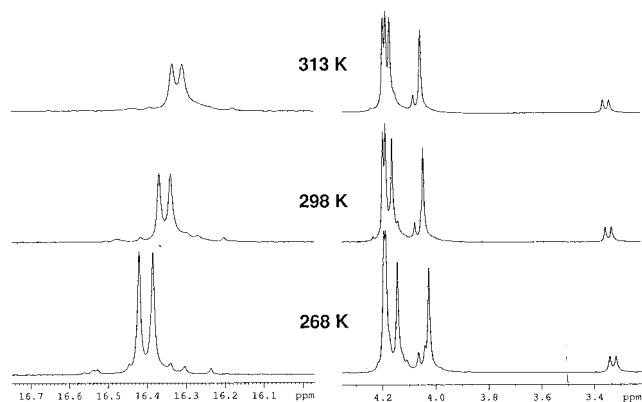

Figure 11. 1D ^{1}H NMR spectra of hypocrellin B doublets and low-field region of th hypocrellin B NMR spectrum as a function of temperature. Line broadening is attributed to intermolecular proton exchange with trace amounts of water.
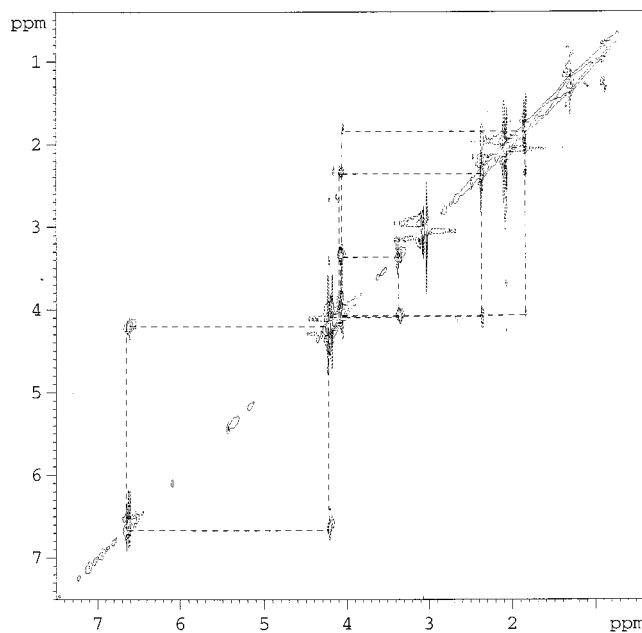

Figure 12. 2D ROESY NMR spectrum of hypocrellin B at 268 K showing all signals except for phenolic hydroxyls. Dashed lines indicate negative contours. Water peaks have been partially removed to clarify the spectrum.

Figure 13. (a) Linear plot of rate constants k for **A → B** (open circles) and **A ← B** (closed circles) processes vs temperature according to the Eyring equation; $r = -0.997$. (b) Linear plot of rate constants k for **B → C** (open circles) and **B ← C** (closed circles) processes vs temperature according to the Eyring equation; $r = -0.999$.

There are at least two ways to respond to this objection. It is possible that the structural changes induced by H-atom transfer do not significantly affect the electronic structure of the tautomeric species in such a way as to destroy the mirror-image symmetry. We had also argued earlier[5,6,12] that the ground state of hypericin is already partially tautomerized or exists in equilibrium between various isomeric species and that this ground-state heterogeneity yields the observed mirror-image symmetry between absorption and emission spectra.
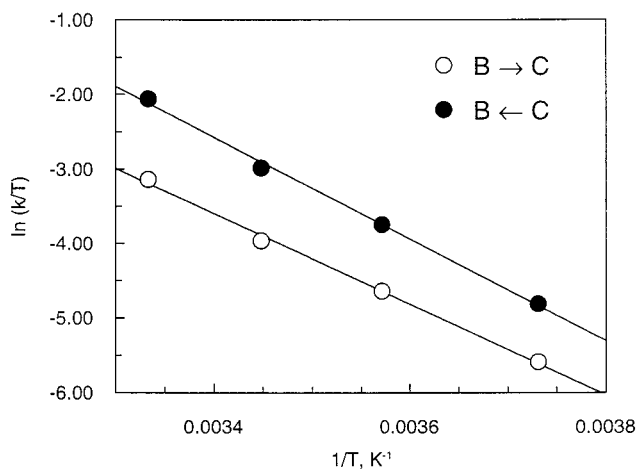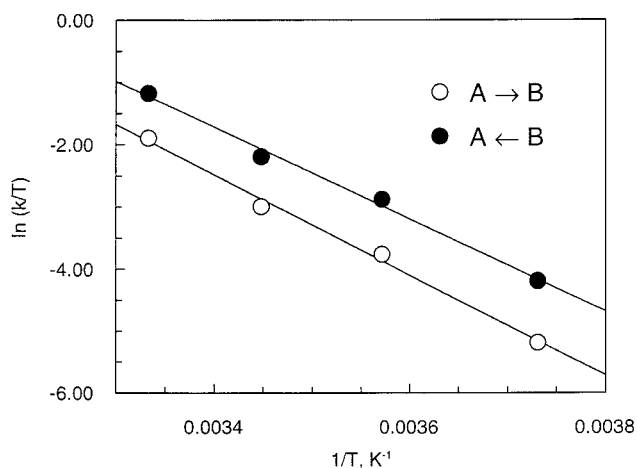
It is of considerable interest that recent ab initio calculations at the RMP2/6-31G(d) level of theory[32] indicate that only the so-called normal form of hypericin is populated at room temperature. In recent transient absorption[7,8] and fluorescence upconversion studies[12] the excited-state kinetics of hypericin depended on the two different excitation wavelengths and the two different emission wavelengths employed. These results were used to confirm the assignment of ground-state heterogeneity in hypericin. Our assignment must be carefully reconsidered in the light of our ab initio calculations and the NMR results presented here. We are currently performing a more exhaustive investigation by measuring the excited-state kinetics with a tunable excitation source.

The ultrafast spectroscopic evidence for ground-state heterogeneity in hypocrellin A is much more convincing. We have
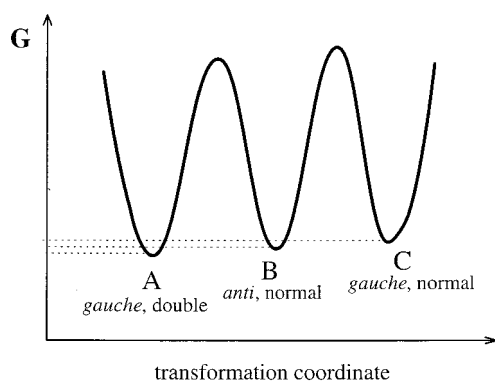
Figure 14. Ground-state energy surface for the three interconverting species **A**, **B**, and **C** of hypocrellin A based on the results of dynamic NMR simulations.

noted that at first glance, the similarity of the structures (Figure 1) and the optical spectra[5–15] of hypericin and hypocrellin would lead one to believe that they should exhibit, at least superficially, similar excited-state photophysics. This is not the case. The time constant for excited-state H-atom transfer in hypericin is ~10 ps and essentially independent of solvent[6,15] whereas for hypocrellin it ranges from 50 to 250 ps in the solvents we have investigated.[10,15] In addition, the H-atom transfer reaction in hypericin exhibits no isotope effect,[6,15] whereas in hypocrellin a small isotope effect of 1.4 is observed.[11,15]

The current picture that we have formed of the excited-state dynamics of hypericin and hypocrellin is that the different photophysical behavior that we have enumerated above of these two structurally very similar molecules arises because we are probing different regions of very similar potential energy surfaces arising from the simultaneous optical excitation of at least two ground-state species.[15] A crucial result in forming this hypothesis is that we resolve a time constant in the hypocrellin photophysics that is comparable to that observed in hypericin. This ~10 ps component in hypocrellin, observed in both transient absorption[15] and fluorescence upconversion measure-

ments[50] unifies our picture of the photophysics of hypericin and hypocrellin if we can interpret it as an excited-state H-atom transfer arising from another tautomeric species and if we can relate it to the corresponding process in hypericin.

Finally, although it has been shown that the antiviral and antitumor activities of hypericin can be dependent on oxygen, comparative studies for nine perylenequinones, including hypocrellin and hypericin, provide evidence, however, that the quantum yield of singlet oxygen formation is not sufficient to explain the reported antiviral activities of these molecules, and that other structural features of perylenequinones are involved.[54] In fact, the quantum yield of singlet oxygen from hypericin is much less than had been presumed initially. Recently, Jardon and co-workers have revised their earlier estimation of a singlet oxygen quantum yield of 0.73,[23] essentially equal to the triplet yield, to 0.36 in ethanol and less than 0.02 in water.[25] Based on this result, mechanisms involving *only oxygen* clearly cannot explain all the activity of hypericin.[51,53] Of special relevance to the role of labile protons for this light-induced biological activity is the observation that hypericin and hypocrellin acidify their surroundings upon light absorption.[14,52,53] The role of photogenerated protons takes on significance in the context of the growing body of literature implicating pH decreases with pharmacologically important functions (see ref 53 and citations therein). A continuing theme of our research is to identify the light-induced photoprocesses responsible for the broad and potent biological activity of these naturally occurring chromophores and to determine their mechanism of action.

Note Added in Proof: A recent NMR study of hypericin in different solvents has been provided by Dax et al. (Dax, T. G.; Falk, H.; Kapinus, E. I. *Monatsh. Chem.* **1999**, *130*, 827−831). This study also concludes that the dominant hypericin species in DMSO is the "normal" form. These workers additionally propose that in tetrahydrofuran the double tautomer is predominant.

JA9906002

(50) Smirnov, A. V.; Das, K.; English, D. S.; Wan, Z.; Kraus, G. A.; Petrich, J. W. *J. Phys. Chem.* In press.

(51) We had previously reported that hypericin does not require oxygen for its antiviral activity (e.g., refs 4, 12, and citations therein). In these cases, however, we were not able to estimate accurately low oxygen levels in our virus samples. We consequently now believe that although the role of oxygen in this activity is significant, the ability of photogenerated protons to enhance or to complement the activity of activated oxygen species is still important (Park, J.; English, D. S.; Wannemuehler, Y.; Carpenter, S.; Petrich, J. W. *Photochem. Photobiol.* **1998**, *68*, 593−597.)

(52) Sureau, F.; Miskovsky, P.; Chinsky, L.; Turpin, P. Y. *J. Am. Chem. Soc*. **1996**, *118*, 9484.

(53) Chaloupka, R.; Sureau, F.; Kocisova, E.; Petrich, J. W. *Photochem. Photobiol.* **1998**, *68*,

(54) Hudson, J. B.; Imperial, V.; Haugland, R. P.; Diwu, Z. *Photochem. Photobiol.* **1997**, *65*, 352−354.